JAREE (2026), Vol. 10, No. 1
doi: 10.12962/jaree.xyzxyz

JAREE Journal on Advanced Research in Electrical Engineering
ISSN: 2579-6216

RESEARCH ARTICLE

Optimal Design Of Bldc Motor Using Abo (African Buffalo Optimization) Algorithm To Minimize Cogging Torque

Irfan Ubaidillah [1] , Feby Agung Pamuji *, Heri Suryoatmojo

[1] Department of Electrical Engineering, Institut Teknologi Sepuluh Nopember, Surabaya, Indonesia
*Corresponding author (feby@ee.its.ac.id).

Received: 12 June 2025; **Revised:** 26 July 2025; **Accepted:** 27 July 2025

Abstract
The increasing use of BLDC motors in recent years indicates rapid development, driven by efforts to reduce pollution through renewable energy. On the other hand, the advantages of BLDC motors have made them particularly attractive, leading to their widespread application not only in the automotive and healthcare sectors but also in aerospace and household appliances. The design of BLDC motors, which utilizes permanent magnets, provides excellent characteristics in terms of power delivery, torque, and efficiency. However, the motor design can sometimes result in uneven torque delivery at certain rotor angles due to cogging torque, which causes the rotor's rotation to become less smooth. The stator design in BLDC motors is a key factor contributing to high cogging torque, as it is influenced by the differences in flux density within the air gap and the interaction between the magnets and the stator surface. This research focuses on reducing cogging torque by optimizing parameters such as magnet height, magnet angle, and slot opening using an optimization method based on the African Buffalo Optimization (ABO) algorithm. The study involves modelling the cogging torque phenomenon through mathematical calculations and optimization using MATLAB. The optimized parameters are then simulated using Ansys Motor CAD software for analysis and evaluation. The research demonstrates that the largest reduction in cogging torque, achieved through ABO optimization, is 48.89%, with comparable results obtained from other benchmark algorithms.

Keywords: air gap, BLDC, cogging torque, desain, optimization

I. Introduction

In recent decades, Brushless DC (BLDC) motors have seen widespread adoption in automotive, aerospace, household, and robotic applications due to their high efficiency, power density, low maintenance, and reliability [1], [2]. These advantages are largely due to their brushless structure and the use of permanent magnets, which minimize energy losses and enhance overall performance.

Despite these benefits, BLDC motors also present several challenges. The use of permanent magnets increases BLDC motors often leads to the occurrence of torque ripple. Torque ripple degrades torque smoothness, causes mechanical vibrations, and generates acoustic noise [1]. One of the primary sources of torque ripple is cogging torque, which arises from the interaction between the rotor magnets and the stator slots during rotation [1], [2], [3], [4]. The rotor topology and the air gap design significantly influence the magnitude of cogging torque.

While control strategies such as current injection have been proposed to suppress it [7], these methods become complex and less effective without optimal motor design. Thus, design-stage optimization is essential to improve motor performance and reliability.

Previous research on BLDC motors includes analytical modelling of geometric effects—such as tooth height, air gap, and magnet dimensions—on cogging torque [1], [5], [6], [7], [8], as well as FEA-based evaluations of design changes [9], [10], [11]. Optimization approaches combining analytical models and metaheuristic algorithms like PSO [2], [12], [13], MOPSO [14], and ANN [15] have also been explored. Other algorithms such as AVOA [16] and Cuckoo Search [14] were tested on slotless BLDC motors.

Recently, the African Buffalo Optimization (ABO) algorithm has gained attention due to its fast convergence and simplicity [17], [18] However, prior studies using ABO focused on single-objective cases or DC motors. This research applies ABO to multi-objective optimization of slotted BLDC motors, targeting reduced cogging torque along with enhanced torque and efficiency.

II. Methods

A. Research Workflow

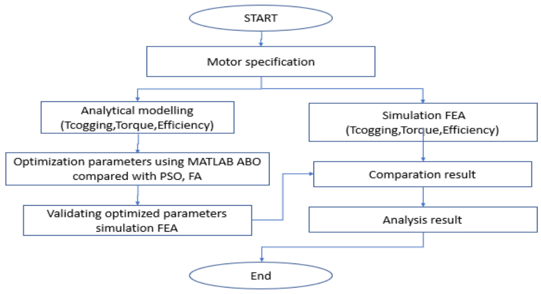

Fig. 1. Research Workflow

In this research, the process starts with motor specification, followed by analytical and FEA simulations.

How to cite: Ubaidillah, I., Pamuji, F. A., & Suryoatmojo, H.. (2026). Optimal Design Of Bldc Motor Using Abo (African Buffalo Optimization) Algorithm To Minimize Cogging Torque. JAREE (Journal on Advanced Research in Electrical Engineering), Volume 10 (No.1).

Optimization is done using ABO and compared with PSO and FA. Results are validated and analyzed to ensure accuracy as in Fig 1.

B. *Motor Specifications*

Existing motor parameters were evaluated using FEA in Ansys MOTOR-CAD, serving as a baseline for performance and optimization comparison. Unoptimized parameters are listed in Table I.

TABLE 1. SIMULATION PARAMETERS

No.	Simulation Parameters		
	Parameter	***Value***	***Units***
1	Air gap (g)	10.515	mm
2	Axial length (L)	60	Mm
3	Magnet arc (Parc)	40	Degree
4	Magnet high (lm)	4.5	mm
5	Slot opening (Sop)	2.18	mm
6	Toth opening (Top)	17.795	mm
7	Toth tip (Ttp)	2.5	mm
8	Toth high (Th)	17.5	mm
9	Toth wide (Wt)	10.5	mm
10	Stator yoke wide (Wsy)	4.35	mm
11	Rotor yoke wide (Wry)	21.15	mm
12	Rotor shaft radius (Rshft)	12.5	mm
13	Rotor radius (Rro)	33.65	mm
14	Motor radius (Rmot)	60	mm
15	Material density (D)	7650	Kg/m3
16	R phase	0.0346	Ohm
17	Current(max)	45	A
18	*Br*	1.401	T
19	μ*r*	1.473	H/m
20	Number of turn coil phase (Nt)	6	

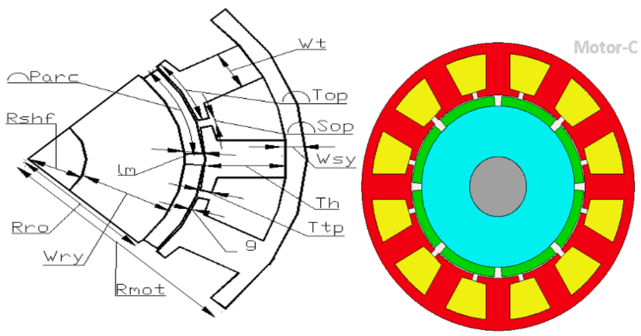

Fig. 2. BLDC Motor Geometry

C. *Purpose of the stud*

The BLDC motor is designed to reduce losses found in conventional DC motors by using a permanent magnet rotor, eliminating the need for brushes. As shown in Fig. 1, it consists of a stator core, stator winding, and rotor. Rotor motion is achieved by alternating current in the stator windings, with speed proportional to the supply frequency. However, slotted stator designs may produce cogging torque—resistive torque caused by rotor alignment with stator slots. This effect, which hinders smooth rotation, is mathematically defined as the change in co-energy with respect to rotor position, as shown in (1).

$$Tcog = -\frac{\partial W(\alpha)}{\partial \alpha} \qquad (1)$$

$$W(\alpha) = \frac{1}{4\mu 0}(R_2^2 - R_1^2)\int_0^L \int_0^{2\pi} G^2(\theta, z)\, B^2(\theta, z)\, d\theta dz \qquad (2)$$

The energy in the stator slots of a BLDC always changes according to the shape of the slots and can be assumed using (2), where G^2 is the relative air gap permeability and B^2 is the relative flux in the air gap[5]

Through [12], the cogging torque equation can be simplified to (3).

$$Tcog(\alpha) = -\frac{L \times Bg^2 Ct}{\mu 0 \pi}(R_2^2 - R_1^2)\sum_{n=1}^{\infty}\left[\frac{1}{n} sin(\frac{n\, Nl\, bo}{2}) sin(\frac{nNl\, \alpha P\, \pi}{Np}) sin(nNl\alpha)\right] \qquad (3)$$

$$Nl = LCM(Ns, NP) \qquad (4)$$

$$Ct = \frac{NsNp}{Nl} \qquad (5)$$

In (3), cogging torque is influenced by the air gap between the rotor's outer and inner radii (*R1, R2*), the least common multiple (LCM) of slots and poles (*Nl*), the rotor magnetic angle ratio (*αP*), and the slot opening angle. Additionally, the air gap flux density (*Bg*), which can be calculated using (7), significantly affects the torque magnitude.

$$Bg = \frac{Am/Ag}{1 + (\mu r \times Kc \times Kl/Pc)} Br \qquad (6)$$

$$Pc = \frac{lm}{g(Am/Ag)} \qquad (7)$$

In (7), the magnet height, magnet surface area (Am), and air gap surface area (Ag) directly influence Bg. In slotted BLDC motors, flux distribution is often non-uniform due to slot geometry, requiring corrections. The linkage factor (8) accounts for flux leakage, while the Carter factor (9) addresses flux spreading at slot edges, with αM as the pole EMF, and τP and τS as pole and slot pitch [15], [19], [20], [21].

$$Kl = 1 + \left(\frac{(4\, lm)}{(\pi \times \mu r \times alpha\_m \times \tau\_p)}\right) ln\left(1\, \pi\, \frac{g}{((1 - \alpha\_m) \times \tau\_p)}\right) \qquad (8)$$

$$Kc = \left(1 - \frac{1}{((\tau\_s / ws) \times (5 \times ((g + lm / \mu r) / ws) + 1))}\right)^2 \qquad (9)$$

From (7) we know that the change of several parameters that affected to Bg are also related to the torque produced, as shown in (10).

$$T = 2 \times Nm \times Nt \times Bgav \times Rro \times L \qquad (10)$$

Where Bgave it the average of Bg. Because of the topology from SPM and BLDC motor design is same, Using the SPM approach, Bgave can be assumed to be no more than 85% of the peak flux (Bg) [21].On the other hand, one of the equally important performance parameters of a BLDC motor is efficiency. Efficiency can be defined as the ratio between the power output and the amount of power wasted, as shown in (11).

$$eff = \frac{Pout}{Pout+Pcopper+Pcore} \quad (11)$$

Where Pout is the output power generated by the motor as in (12) and Pcopper is the losses of the conductor phase when the current flow.

$$Pout = T \times \omega \quad (12)$$

$$Pcopper = 3 \times Rph \times Irms^2 \quad (13)$$

Meanwhile, Pcore is the power loss generated when the material is working[15], [19]. These losses consist of hysteresis losses, material losses, and eddy current losses as shown in equation below.

$$Pcore = Ph + Pc + Pe \quad (14)$$

$$Ph = Kh \times f \times (Bm)^2 \quad (15)$$

$$Pc = Kc \times f \times (Bm)^2 \quad (16)$$

$$Pe = Ke \times f \times (Bm)^{1.5} \quad (17)$$

Where *Kh, Kc,* and *Ke* are constants, f is the operating frequency of the machine, and Bm is the flux density generated in the material.
Based on the characteristic constant from Ansys Motor-Cad material, a graph of the magnetic peak changes generated with losses in the M350-50A material can be calculate, as shown in Fig. 2.

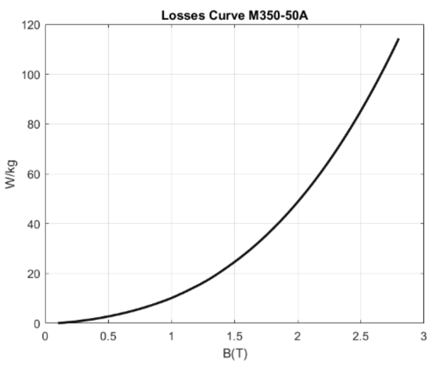

Fig. 3. Losses Curve of M350-50A.

In Fig. 3, losses in material can be found through the mass of the material, which can be calculated using the following equation.

$$Mrotor = Pi \times (Rro^2 - (Rro^2)) \times D \times L \quad (18)$$

$$Mstator = Pi \times (Rmo^2 - (Rro + lm + g + Th - Ttp)^2) \times D \times L \quad (19)$$

$$Mtoth = Ns \times ((Th - Ttp) \times D \times L) + (Ttp \times Top \times D \times L)) \quad (20)$$

Meanwhile, to calculate the flux density on the teeth (Bt) and stator yoke (Bsy), (21) and (22) are used. Then, on the rotor yoke, the mass is calculated using (23).

$$Bry = \frac{\pi \times (Rro+lm) \times Bg}{\mathrm{Ns} \times Wry \times Kst} \quad (21)$$

$$Bsy = \frac{\pi \times (Rro+lm) \times Bg}{\mathrm{Ns} \times Wsy \times Kst} \quad (22)$$

$$Bt = \frac{2\pi \times (Rro+lm) \times Bg}{\mathrm{Ns} \times Wt \times Kst} \quad (23)$$

In the equation above, *Kst* is the stacking factor, which usually ranges from 0.8 to 0.99 [19]

D. BLDC optimization

In this study, optimization is carried out on several selected design parameters of a slotted BLDC motor, based on the analytical formula discussed previously. The parameter optimization is performed using the African Buffalo Optimization (ABO) algorithm, and the results are compared with other algorithms such as Particle Swarm Optimization (PSO) due to the performance and popularity in motor optimization and the Firefly Algorithm (FA) due to the popularity in control application and ability in multi objective problem[22], [23]. The selected design parameters and their constraints are summarized in Table 2.

TABLE 2. PARAMETER WILL BE OPTIMIZED

no	Parameter will be Optimized		
	Parameter	***Range***	***Unit***
1	Magnet heigh (lm)	2-5	Mm
2	Opening slot (Sop)	1-4	Mm
3	Magnet arc (Parc)	38-44	Degree

The total size of outer rotor diameter size was limited and has fixed value, so that it did not change the diameter of the stator and air gap. The purpose of optimizing these parameters was to determine the appropriate parameters to improve the initial design with the aim of reducing cogging torque while minimizing the reduction in torque and efficiency caused by, as shown in the table 3.

TABLE 3. OBJECTIVE FUNCTION

no	Objective Function		
	Function	***Target***	***unit***
1	Cogging Torque	Min	mm
2	torque	Max	mm

no	Objective Function		
	Function	***Target***	***unit***
3	Efficiency	Max	degree

E. ABO (African Buffalo Optimization)

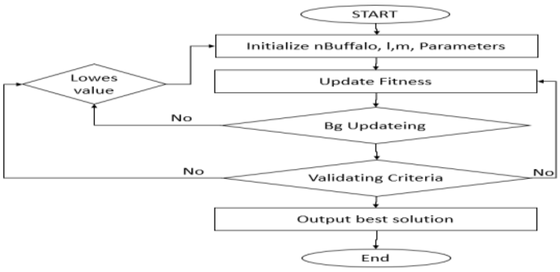

Fig. 4. ABO Flow Chart

In the main process of optimization in this paper used one of the latest methods is African Buffalo Optimization (ABO). Basically, ABO is based on the natural phenomenon of buffalo in Africa. The concept of this optimization method is taken from the habits of African buffalo, which optimally group together to find and determine the location of their food based on their hearing and sounds. ABO was developed to provide a method that is not only reliable and accurate but also efficient and easy to use. In (24) and (25), *"wk"* represents the call *"waa,"* indicating the function to explore new locations by buffalo k. Meanwhile, 'mk' is defined as the call "maa," which commands exploitation at the discovered location. Meanwhile, wk' and mk' are commands to further explore and exploit.

while l and m are learning parameters and λ is value [0,1]. To determine the steps for further exploration and exploitation, the algorithm will stop when the criterion *bg* (best location relative to the global optimum) is met [17].

$$mk' = mk + m(bg - wk) + l(bpk - wk) \qquad (24)$$

$$wk' = \frac{(wk+mk)}{\lambda} \qquad (25)$$

III. Results and Discussion

A. Simulaton before Optimization

As an initial reference, a simulation was performed on the baseline design parameters of the BLDC motor using Ansys Motor-CAD. This initial simulation allowed the estimation of the cogging torque generated by the motor. The input parameters used in the baseline model are listed in Table I,

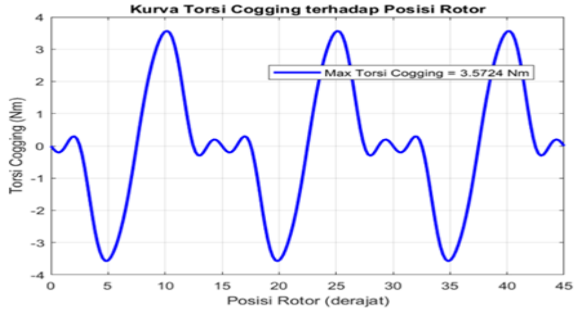

Fig. 5. Cogging Torque before optimized.

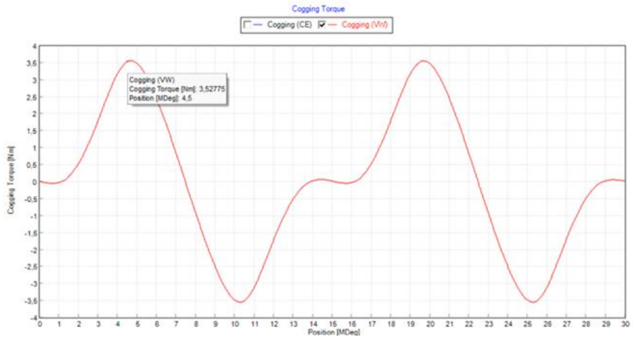

Fig. 6. FEA Cogging torque before optimized

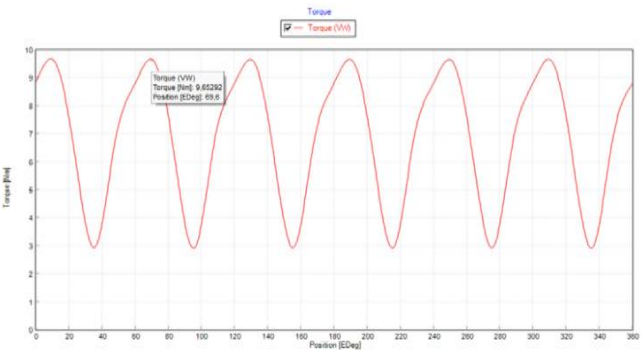

Fig. 7. FEA Torque before optimized

The cogging torque result is shown in Fig. 6, where the cogging torque was found to be 3.5277 Nm, with a maximum torque ripple of 9.6529 Nm. Meanwhile, the MATLAB simulation yielded a similar result, with a cogging torque of approximately 3.5724 Nm.

B. Case 1: Optimization with Weight Sum

In the first case, optimization was performed using ABO as the main algorithm with the addition of the Weighted Sum method to define the objective function. Before The selection of parameters l and m in the ABO algorithm was done by testing several parameters and then plotting them using grid search to find the best parameters, as shown in Fig. 8. The best result was obtained at *l=1.2,* and *m=0.7*, indicated by the darkest colour.

Fig. 8. Grid search for best l and m.

```
1.  Set parameters: { Nbufallo,itertion= 150,m = 0.7, l = 1.2 ,λ=1}
2.  Randomly initialize each buffalo's position within [lm, g, Parc]
3.  Evaluate fitness based on f  in Equation (26)
4.  Store current position as memory (mem) and best fitness
6.  Determine global best buffalo (gBest)
7.   iteration =>> For each buffalo i
8.       Compute movemen Δ = m * (mem(i) - pos(i)) + l * (gBest - pos(i))
9.      Update position:
          newPos = pos(i) + Δ
10.      Apply boundary limits to newPos
12.      Evaluate new fitness f(i)
13.      If f(i) < bestFit(i) then
14.         Update mem(i) = newPos
15.         Update bestFit(i) = f(i)
16.      End if
17.      Update pos(i) = newPos and fit(i) = f(i)
18.    End for
19.    If current best fitness < gBestFit
20.      Update gBest = current best position
21.      Update gBestFit = current best fitness
22.    End if
```

Fig. 9. ABO Pseucode optimizing.

Objective function in Fig. 9 is combined using the weighted-sum method, as shown in (26), to prioritize objectives[13], [24]. Weights x,y,z are assigned based on sensitivity analysis, reflecting each objective's influence. Torque and cogging torque show greater variation than efficiency. Final weights are: x=0.04887(torque), y=0.5076 (cogging torque), and z=0.0036 (efficiency).

The sampling of parameter combinations is performed using the Latin Hypercube Sampling (LHS) method, which efficiently generates well-distributed input samples across the design space by dividing parameter ranges into equal intervals and selecting values randomly within each [24]. In this study, each parameter was divided into 10 intervals.

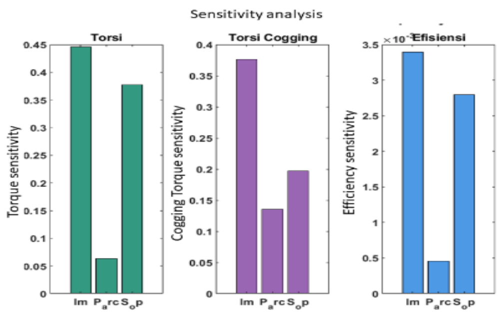

Fig. 10. Sensitifity analysis.

Since optimization algorithms typically minimize objective functions, functions aimed at maximization are reformulated as $1 - fnorm$, where $fnorm$ represents the normalized form of each function, scaled to a [0, 1] range. The final objective function f is then constructed using this normalized and inverted form.

$$f = \big(X * (1 - Tnorm)\big) + (Y * Coggingnorm) + \big(Z * (1 - Efisiensinorm)\big) \quad (26)$$

$$Tnorm = (T(x) - Tmin)/(Tmax - Tmin) \quad (27)$$

The maximum and minimum values used for normalization are obtained from the sample data generated using the previously applied Latin Hypercube Sampling (LHS) method.

The simulation results of ABO using the weighted sum method were compared with Finite Element Analysis (FEA) results to evaluate accuracy and performance. The torque obtained from MATLAB simulation was 1.7895 Nm, as in Fig. 11.

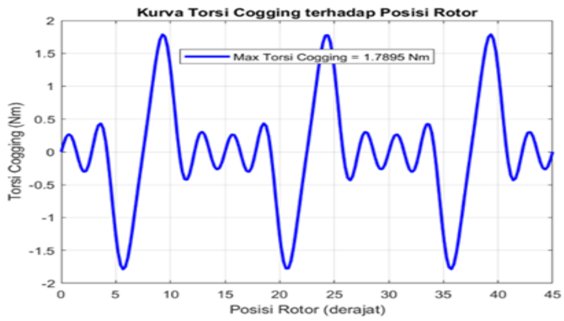

Fig. 11. ABO optimized Cogging Torque

Its also showing a small error of 0.59% compared to the initial FEA result of 1.80015 Nm. However, this value represents a 48.87% reduction compared to the original torque before optimization. For average torque, the result increased slightly by 0.354%, from 6.8208 Nm to 6.845 Nm , although with a 3.21% error from MATLAB result against FEA. The efficiency achieved through ABO was 89.603%, slightly lower than the initial efficiency of 90.157%, despite a 1.62% error when compared with the FEA result from MTLAB result. Overall, the ABO approach effectively improved efficiency and slightly enhanced maximum torque, while significantly reducing cogging torque.The comparation can bee seen in table 4.

TABLE 4. ABO WITH WEIGHT SUM RESULT

ABO with weight sum result					
Obj	***MATLAB***	***FEA Optimized***	***FEA Before***	***Error MATLAB***	***FEA rise/drop***
Torque Cogging	1.7895 Nm	1.80015 Nm	3.5227 Nm	0.59%	(-) 48.87 %
Torque ave	7.0648 Nm	6.845 Nm	6.8208 Nm	3.21%	(+) 0.354 %
Efficiency	91.061 %	89.603 %.	90.157 %	1.62%	(-) 0.614 %
Max Torque		9.2872 Nm	9.652 Nm		(-) 3.72 %

The results in the table above were obtained using the optimized values of lm = 3.6751 mm, Parc = 44 degrees, and Sop = 2.3339 mm. These optimized parameters yield performance values that are comparable to those obtained using the benchmark algorithms, as shown in table 5..

TABLE 5. OPTIMIZED PARAMETERS COMPARATION

No	Optimized parameters comparation			
	Optimized Parameters	***ABO***	***PSO***	***FA***
1	Lm (mm)	3.6751	3.6737	3.6726
2	Parc (degree)	44	44	44
3	Sop (mm)	2.3339	2.3353	2.3358

The optimization results based on the selected parameters also demonstrate a nearly identical reduction in cogging torque, as presented in the following table 6. This similarity in results from ABO, PSO, and FA are likely due to the fact that the three optimized parameters converged to the same or nearly identical optimal values.

TABLE 6. MATLAB RESULT CASE 1

no	MATLAB result case 1			
	Obj Function	***ABO***	***PSO***	***FA***
1	Torsi Cogging	1.7895 Nm	1.7901 Nm	1.7901 Nm
2	Torsi	7.0648 Nm	7.0648 Nm	7.0645 Nm
3	Efisiensi	91.061%	91.062%.	91.0613%.

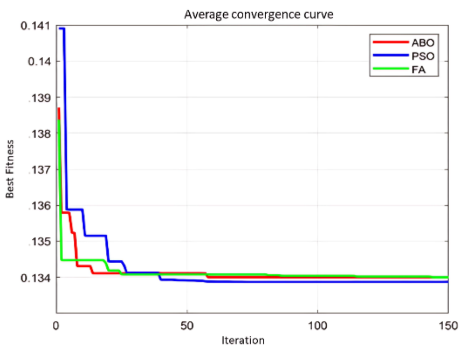

Fig. 12. Best finess convergency curve

From Fig. 12, the convergence curves show that all algorithms rapidly improve in early iterations. FA converges fastest, followed by ABO and PSO. Despite similar final fitness values, ABO demonstrates smoother and more stable convergence than PSO, indicating its reliability and competitive performance.

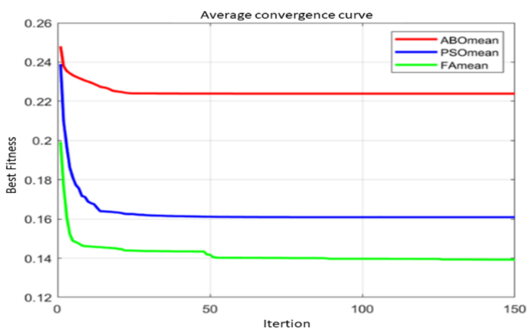

Fig. 13. Average Convergency curve

The graph above shows the average fitness values over 40 independent runs. It can be observed that FA demonstrates the most stable performance, consistently achieving the lowest average fitness values. However, ABO offers advantages in terms of faster convergence speed, wider exploration capability, and the shortest processing time among the three algorithms, as summarized in the table 7.

TABLE 7. ALGORITHM PERFORMANCE CASE 1

no	Algorithm performance case 1.				
	Algorithm	***Mean Fitness***	***Best Fitness***	***Time Average***	***Std Deviation***
1	ABO	0.2239	0,1340	0.3695 s	0.0787
2	PSO	0.1609	0.1338	0.4277 s	0.0437
3	FA	0.1392	0.1339	6.519 s	0.0179

C. Case II: Optimization using ABO with Pareto Filter

In this second case, ABO testing was also conducted by adding a Pareto filter as shown in Fig. 4 to determine the best solution. Unlike first case, in this simulation, no weights were used for each objective function that became the optimization goal, so that the objective functions were only *F(1) = T cogging*, *F(2) = - Torque*, and *F(3) = - eff*. The minus sign was used because the function would be maximized.

```
Set parameters: { Nbufallo,itertion= 150,m = 0.7, l = 1.2, λ=1 }
Randomly initialize each buffalo's position within [lm, g, Parc]
Evaluate fitness based on f
Store current position as memory (mem) and best fitness
Determine global best buffalo (gBest)
  iteration =>> For each buffalo i
      Compute movemen Δ = m * (mem(i) - pos(i)) + l * (gBest - pos(i))
      Update position:
        newPos = pos(i) + Δ
      Apply boundary limits to newPos
      Evaluate new fitness f(i)
      If f(i) < bestFit(i) then
         Update mem(i) = newPos
         Update bestFit(i) = f(i)
      End if
    Update global best (gBest) if better solution is found
    Save T, Tcog, eff, and gBest to results
Apply Pareto filtering to get non-dominated solutions
   if all(f(j,:) <= f(i,:)) && any(f(j,:) < f(i,:)) // dominating condition
      Get non- dominated solution from all pareto front
   End if
```

Fig. 14. ABO with Pareto filter Pseucode

These functions(*F*) are then selected to determine which solutions do not dominate the others using (28). A function is said to dominate another function if it is better or equal, and significantly better in at least one aspect compared to the other function.

$$\boldsymbol{F_j} \prec \boldsymbol{F_i}, \text{if} \forall k \in \{1,2,\dots,m\},\ F_j^{(k)} \leq F_i^{(k)} \text{ and }$$
$$\exists k \in \{1,2,\dots,m\},\ F_j^{(k)} < F_i^{(k)} \qquad (28)$$

The non-dominated solutions obtained by ABO are represented in the Pareto front shown in Fig. 15, with red points indicating the best trade-off solutions. For comparison, Pareto fronts generated by PSO and FA are illustrated in Fig. 16 and Fig. 17, respectively.

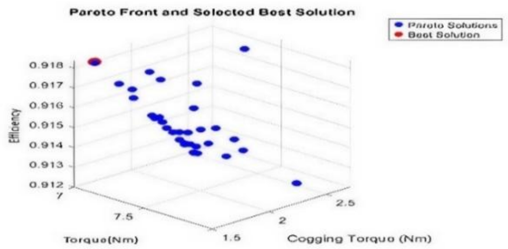

Fig. 15. ABO pareto solution

The Pareto fronts of ABO, PSO, and FA illustrate their performance in optimizing torque, cogging torque, and efficiency. ABO demonstrates the most balanced results, with dense and evenly distributed solutions indicating strong exploration and exploitation.

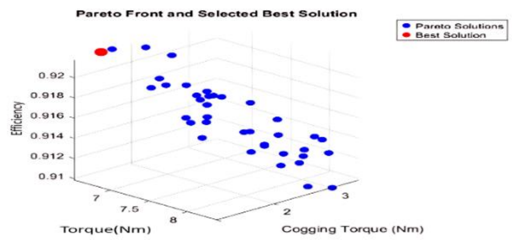

Fig. 16. PSO Pareto Solution

PSO shows a broader spread, reflecting higher diversity but less stability, with some solutions achieving low cogging torque at the cost of reduced efficiency. In contrast, FA produces a narrower Pareto front with clustered solutions, suggesting limited exploration.

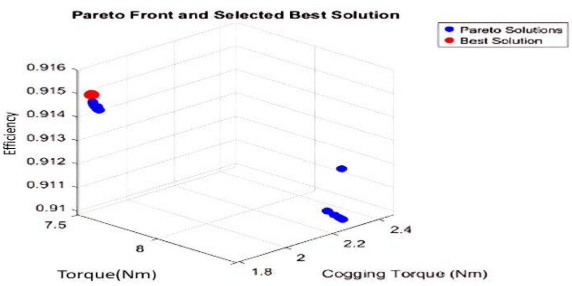

Fig. 17. FA Pareto Solution

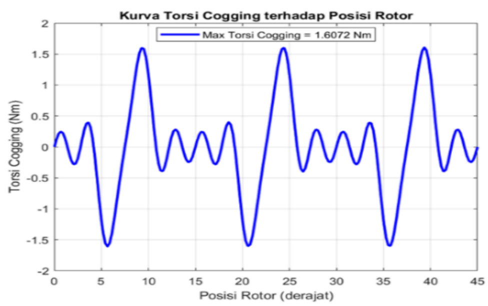

Fig. 18. Matlab Torque Cogging ABO Optimized with Pareto Filter

TABLE 8. ABO WITH PARETO FILTERING RESULT

ABO with Pareto filtering result					
Obj	***MATLAB***	***FEA***	***FEA Awal***	***Error% MATLAB***	***FEA rise/drop***
Torsi Cogging	1.6075 Nm	1.74283 Nm	3.5227 Nm	7.76%	(-) 50.5%
Torsi ave	6.812 Nm	6.66 Nm	6.8208 Nm	2.28%	(-) 2.35%
Efisiensi	9.8%	89.903 %.	90.157 %	2.11%	(-) 0.281%
Max Torsi		8.96 Nm	9.652 Nm		(-) 7.16 %

Table 8 presents the ABO results with Pareto filtering validated by FEA. Cogging torque was reduced by 50.5%, while average torque and efficiency slightly decreased by 2.35% and 0.28%, respectively. Maximum torque dropped by 7.16%, reflecting a trade-off between peak and smooth operation. MATLAB predictions showed good agreement with FEA, with errors ranging from 2.11% to 7.76%, which are higher than those from the previously discussed using weight sum method.

TABLE 9. ABO WITH PARETO FILTERING RESULT

no	MATLAB result case 2			
	Obj Function	***ABO***	***PSO***	***FA***
1	Torsi Cogging	1.6075 Nm	1.4721Nm	1.8345 Nm
2	Torsi	6.812 Nm	6.533 Nm	7.5630Nm
3	Efisiensi	91.8%	92.18%.	91.5%.

Compared to PSO and FA, ABO achieves a more balanced outcome low cogging torque (1.61 Nm), high torque (6.81 Nm), and high efficiency (91.8%). While FA yields the highest torque, it has higher cogging and lower efficiency. PSO offers better efficiency but lower torque. This confirms ABO's strength in achieving well-compromised performance.

TABLE 10. ABO WITH PARETO FILTERING RESULT

no	Optimized parameters comparation			
	Optimized Parameters	***ABO***	***PSO***	***FA***
1	Lm (mm)	2.819	2.066	3.772
2	Parc (degree)	44	43,89	44
3	Sop (mm)	2.36	2.377	2.379

IV. CONCLUSION

This study demonstrates the effectiveness of the African Buffalo Optimization (ABO) algorithm in the multi-objective optimization of BLDC motor design. In comparison with PSO and FA, ABO achieves a competitive fitness value (0.1340), fast average computation time (0.3695 seconds), and the widest exploration range as indicated by the highest standard deviation (0.0787). While PSO offers the most stable convergence and FA shows slower performance, ABO provides a balanced trade-off between speed, accuracy, and solution diversity.

In the first experiment, all three algorithms yielded similar optimal solutions. In the second case, where Pareto filtering was applied, ABO and PSO produced more diverse and distributed Pareto fronts than FA. Furthermore, simulation results showed that ABO successfully reduced cogging torque by up to 48.87% and 50,5% from its initial value, with minimal error (0.59%) and (7.76%) between MATLAB predictions and FEA validation. These findings confirm that ABO is not only accurate but also computationally efficient, making it highly suitable for BLDC motor design involving multi-objective optimization specially combined with wight sum method.

Acknowledgment

The author would like to thank the Energy Conversion Laboratory and the supervisors who assisted in this research.

References

[1] A. J. Kanapara and K. P. Badgujar, "Performance improvement of permanent magnet brushless DC motor through cogging torque reduction techniques," in *2020 21st National Power Systems Conference, NPSC 2020*, Institute of Electrical and Electronics Engineers Inc., Dec. 2020. doi: 10.1109/NPSC49263.2020.9331855.

[2] C. Kamal, T. Thyagaranaj, M. Selvakumari, and D. Kalpana, "Cogging torque minimization in brushless DC motor using PSO and GA based optimization," in *2017 Trends in Industrial Measurement and Automation (TIMA)*, Chennai, China: [IEEE], Oct. 2017. doi: 10.1109/TIMA.2017.8064815.

[3] T. Jhankal and A. N. Patel, "Cogging Torque Minimization of High-Speed Spoke-Type Radial Flux Permanent Magnet Brushless DC Motor Using Core Bridge Width Variation Technique," in *2023 International Conference on Recent Advances in Electrical, Electronics and Digital Healthcare Technologies, REEDCON 2023*, Institute of Electrical and Electronics Engineers Inc., 2023, pp. 750–755. doi: 10.1109/REEDCON57544.2023.10151443.

[4] T. A. Anuja, M. Arun Noyal Doss, R. Senthilkumar, K. S. Rajesh, and R. Brindha, "Modification of Pole Pitch and Pole Arc in Rotor Magnets for Cogging Torque Reduction in BLDC Motor," *IEEE Access*, vol. 10, pp. 116709–116722, 2022, doi: 10.1109/ACCESS.2022.3217233.

[5] L. Zhu, S. Z. Jiang, Z. Q. Zhu, and C. C. Chan, "Analytical methods for minimizing cogging torque in permanent-magnet machines," *IEEE Trans Magn*, vol. 45, no. 4, pp. 2023–2031, Apr. 2009, doi: 10.1109/TMAG.2008.2011363.

[6] L. B. Jing, L. Liu, R. H. Qu, Q. X. Gao, and Z. H. Luo, "A novel method of reducing the cogging torque in SPM machine with segmented stator," *Journal of Electrical Engineering and Technology*, vol. 12, no. 2, pp. 718–725, Mar. 2017, doi: 10.5370/JEET.2017.12.2.718.

[7] T. Alberto and O. Matteo, "A new method for the analytical determination of the complex relative permeance function in linear electric machines with slotted air gap," in *2016 International Symposium on Power Electronics, Electrical Drives, Automation and Motion (SPEEDAM)*, IEEE, Jun. 2016. doi: 10.1109/SPEEDAM.2016.7525884.

[8] J. Xintong, X. Jingwei, L. Yong, and L. Yongping, "Theoretical and simulation analysis of influences of stator tooth width on cogging torque of BLDC motors," *IEEE Trans Magn*, vol. 45, no. 10, pp. 4601–4604, 2009, doi: 10.1109/TMAG.2009.2022639.

[9] B. Arvind Kumar, C. Kamal, D. Armudhavalli, and T. Thyagarajan, "Reformed Stator Design of BLDC Motor for Cogging Torque Minimization Using Finite Element Analysis," in *2018 4th International Conference on Electrical Energy Systems (ICEES)*, Chennai, India: IEEE, Aug. 2018. doi: 10.1109/ICEES.2018.8442389.

[10] S. Rudy, W. Herlina, and S. P. Yudha, "Reduction of Cogging Torque on Brushless Direct Current Motor with Segmentation of Magnet Permanent," in *2017 4th Int. Conf. on Information Tech., Computer, and Electrical Engineering (ICITACEE)*, Semarang, Indonesia: IEEE, Jan. 2017. doi: 10.1109/ICITACEE.2017.8257680.

[11] V. Bogdan, M. Adrian, L. Leonard, B. Alexandra, S. Alecsandru, and N. Ionut, "Design and Optimization of a BLDC Motor for Small Power Vehicles," in *SIELMEN 2021 - Proceedings of the 11th International Conference on Electromechanical and Energy Systems*, Institute of Electrical and Electronics Engineers Inc., 2021, pp. 438–443. doi: 10.1109/SIELMEN53755.2021.9600327.

[12] L. Zhang, B. Tang, S. Tan, and X. Ning, "Cogging Torque Reduction of Permanent Magnet Motor Based on Particle Swarm Optimization Algorithm," in *Journal of Physics: Conference Series*, Institute of Physics, 2022. doi: 10.1088/1742-6596/2404/1/012046.

[13] N. Umadevi, M. Balaji, and V. Dr. Kamaraj, "Design Optimization of Brushless DC Motor using Particle Swarm Optimization," in *2014 IEEE 2nd International Conference on Electrical Energy Systems (ICEES)*, Chennai, India: IEEE, Oct. 2014. doi: 10.1109/ICEES.2014.6924153.

[14] M. Niaz Azari, M. Samami, and S. M. Abedi Pahnehkolaei, "Optimal design of a brushless DC motor, by using the cuckoo optimization algorithm," *International Journal of Engineering, Transactions B: Applications*, vol. 30, no. 5, pp. 668–677, May 2017, doi: 10.5829/idosi.ije.2017.30.05b.06.

[15] S. A. Sadrossadat and O. Rahmani, "ANN-based method for parametric modelling and optimising efficiency, output power and material cost of BLDC motor," *IET Electr Power Appl*, vol. 14, no. 6, pp. 951–960, Jun. 2020, doi: 10.1049/iet-epa.2019.0686.

[16] S. N. Tripathy, S. Kundu, A. Pradhan, and P. Samal, "Optimal design of a BLDC motor using African vulture optimization algorithm," *e-Prime - Advances in Electrical Engineering, Electronics and Energy*, vol. 7, Mar. 2024, doi: 10.1016/j.prime.2024.100499.

[17] J. B. Odili, A. Noraziah, B. Alkazemi, and M. Zarina, "Stochastic process and tutorial of the African buffalo optimization," *Sci Rep*, vol. 12, no. 1, Dec. 2022, doi: 10.1038/s41598-022-22242-9.

[18] R. Ullah Khan, B. Bhattacharyya, and G. Singh, "A novel African buffalo optimization for the minimization of cogging torque in modified permanent magnet DC motor," *Sustainable Energy*

Technologies and Assessments, vol. 46, Aug. 2021, doi: 10.1016/j.seta.2021.101240.

[19] D. C. Hanselman, *Brushless Permanent Magnet Motor Design Second Edition*, 2nd ed. Lebanon, Ohio: Magna Physics Publishing, 2006.

[20] J. Zhao and Y. Yu, "Brushless DC Motor Fundamentals Brushless DC Motor Fundamentals Application Note," 2011. [Online]. Available: www.MonolithicPower.com

[21] Juha. Pyrhonen and Tapani. Jokinen, *Design of Rotating Electrical Machines*. John Wiley & Sons, 2009.

[22] S. Bazi, R. Benzid, Y. Bazi, and M. M. Al Rahhal, "A fast firefly algorithm for function optimization: Application to the control of bldc motor," *Sensors*, vol. 21, no. 16, Aug. 2021, doi: 10.3390/s21165267.

[23] M. Manoj Kumar and N. Prema Kumar, "PSO and Firefly Algorithms based control of BLDC motor drive," in *2nd International Conference on Inventive Systems and Control*, Coimbatore, India: Institute of Electrical and Electronics Engineers, Jul. 2018, p. 908. doi: 10.1109/ICISC.2018.8398951.

[24] Z. Wang, J. Gong, and B. Liu, "Multi-objective optimization of the hollow shaft direct drive motor," *Advances in Mechanical Engineering*, vol. 15, no. 3, Mar. 2023, doi: 10.1177/16878132231163079.